Forensic Science International 379 (2026) 112774

Contents lists available at ScienceDirect

Forensic Science International

journal homepage: www.elsevier.com/locate/forsciint

Design of experiments (DOE) analysis of the effects of environmental conditions on bloodstain degradation using spectroscopic methods

Laurianne Huard [a,b,*], Frank Crispino [a,b,c], Cyril Muehlethaler [a,b,c,**]

[a] University of Quebec at Trois-Rivières, Canada
[b] Groupe de Recherche en Science Forensique (GRSF), Trois-Rivières, Canada
[c] Centre International de Criminologie Comparée (CICC), Montreal, Canada

ARTICLE INFO

Keywords:
Bloodstain
Degradation
Near-Infrared
Raman
Hyperspectral Imaging
Design of Experiments
Principal Component Analysis

ABSTRACT

Blood is one of the most common types of trace found at crime scenes. However, from a forensic point of view, the potential of blood traces is still not fully exploited, as there is as yet no reliable technique for dating blood traces found at scenes. The same difficulties are cited in the literature for published research on blood traces: the mechanisms of blood degradation are known and validated, but traces found at scenes are not controlled samples. Traces therefore need to be evaluated in the light of this uncertainty and the factors that can influence the blood trace dating model. In the course of this project, we assessed the significance of the environmental effects of temperature (10–40°C), humidity (25–75 %) and radiation (none and maximum) using three different spectroscopic techniques: Raman spectroscopy, MicroNIR spectroscopy and hyperspectral imaging. The use of a climatic chamber with the addition of LED lamps (daylight and UV) enabled parameters to be controlled during a 3-day aging period for each sample. By means of a 2-level experimental screening design of the three factors, we were able to observe complementarity between the methods used. Raman spectroscopy highlighted the influence of temperature, MicroNIR spectroscopy provided information on the influence of temperature and relative humidity, and hyperspectral imaging demonstrated the influence of temperature and the presence of radiation. These results provide a better understanding of the factors that cause the blood degradation model to deviate, enabling us to develop a more comprehensive model of these factors.

1. Introduction

The question of time and the dating of traces has long fascinated experts. Forensic scientists attempt to reconstruct past events, with the use of the physicochemical properties of the traces found [1]. They can therefore show an association between a trace and a source, or even between a trace and an activity. The question of precisely dating the moment of the deposition of a trace, however, is much more complicated. A difference of a few days can make it possible to distinguish between a trace linked to the crime or, on the contrary, a lawful deposition made prior to the crime, and experts are currently at a loss as they cannot estimate the time interval precisely. This is all the more important as blood is one of the most common types of traces found at crime scenes [2]. From a forensic point of view, the potential of blood traces has yet to be fully exploited [1]. Despite some advances in this field in recent years by various research groups [1,3–18], there is still no reliable technique for the estimation of the time since deposition of blood traces found at crime scenes. This problem is even cited in the specialized literature as the quest for the Holy Grail [1]. Indeed, an accurate estimate of the age of a bloodstain could provide a temporal link between the trace and the commission of a crime and reinforce the weight of evidence through a unity of time, place, and action [19].

A bloodstain undergoes several physicochemical transformations during the degradation process, mainly: a change in color from red to dark brown, a change in hemoglobin configuration, and a physical change in the red blood cells [2]. Since these changes are time-dependent, the proportions of different hemoglobin configurations can be used to estimate the age of a bloodstain. This process begins as soon as the blood is exposed to air, i.e., as soon as it leaves the body (*ex vivo*). The initial changes consist of the evaporation of the water

* Correspondence to: University of Quebec at Trois-Rivières, Department of Chemistry, Biochemistry and Physics, 3351 Boulevard des Forges, CIPP-2134, Trois-Rivières, QC G9A5H7, Canada.
** Corresponding author at: University of Quebec at Trois-Rivières, Canada.
E-mail addresses: Laurianne.huard@uqtr.ca (L. Huard), cyril.muehlethaler@uqtr.ca (C. Muehlethaler).

https://doi.org/10.1016/j.forsciint.2025.112774
Received 4 July 2024; Received in revised form 8 December 2025; Accepted 14 December 2025
Available online 16 December 2025

contained in the blood, followed by coagulation, which increases viscosity [20]. Once the water has evaporated, the red blood cells form the majority of the dry bloodstain, and these are composed of 90 % hemoglobin [2]. Changes in hemoglobin therefore make up most of the blood degradation process and is the target compound for the evaluation of bloodstain degradation. These changes consist firstly of the saturation of deoxyHB (deoxyhemoglobin) into oxyHB (oxyhemoglobin) on contact with ambient oxygen, followed by the auto-oxidation of oxyHB to metHB (methemoglobin). The denaturation step that follows is a conformational change of metHB to form hemochromes and hemichromes [21,22]. This step is reversible with rehydration of the blood [23]. Therefore, this denaturation is more likely to occur when humidity is low. Knowledge of the *ex vivo* blood degradation process is still superficial, so the duration of each of these steps remains unknown. Fig. 1 below illustrates the hemoglobin degradation process.

Published research on bloodstain dating have all faced the same difficulties: the physico-chemical principles of degradation are known and validated, and laboratory models tend to show a good relationship between time-since-deposition and degradation [3,4,8,13–16,24]. However real-life traces are not controlled samples whose properties are known and mastered. On the contrary, they are often deposited under chaotic conditions (aggression, murder), and are very often imperfect, of poor quality, contaminated and/or degraded. Previous studies have shown that the direct environment of traces (indoor/outdoor, temperature, humidity, wind, etc.) has a major and direct influence on degradation dynamics, making it very difficult to develop accurate models for the evaluation of the time since deposition [3,5,16,17]. Bloodstain traces must be evaluated with this uncertainty in mind since the sequence of events is unknown and we often do not know what might have happened between the time of deposition and the time of detection.

With these considerations in mind, we sought to do the opposite of previous publications, namely to study blood degradation under more extreme environmental conditions, to see which responses are stable and which analytical techniques are better suited to highlight them. This project therefore aims to assess the influence of temperature, relative humidity, and radiation on the degradation of blood traces, by three common spectroscopic techniques, respectively hyperspectral imaging, Raman spectroscopy and near-infrared spectroscopy through a design of experiments (DoE) evaluation. An understanding of how the upper and lower limits of these environmental factors affect the bloodstain degradation could enable us to improve our understanding of the degradation mechanisms and learn how laboratory models of degradation deviate from real-life traces. This results in a broader model adapted to changing conditions, instead of an overly precise model that no longer works under different environmental conditions.

A second objective of this project is to compare the performances of common spectroscopic analysis methods for the analysis of bloodstain degradation, namely near infrared spectroscopy (MicroNIR), Raman spectroscopy and hyperspectral imaging. These techniques are fast, simple, and non-destructive, and have the advantage of being portable. We intend to show the complementarity of these techniques using a fractional factorial design of experiments, which will enable us to highlight the features responsible for degradation and which will enable us to highlight the features involved in degradation, their significance, and any two-to-one or three-to-one interactions.

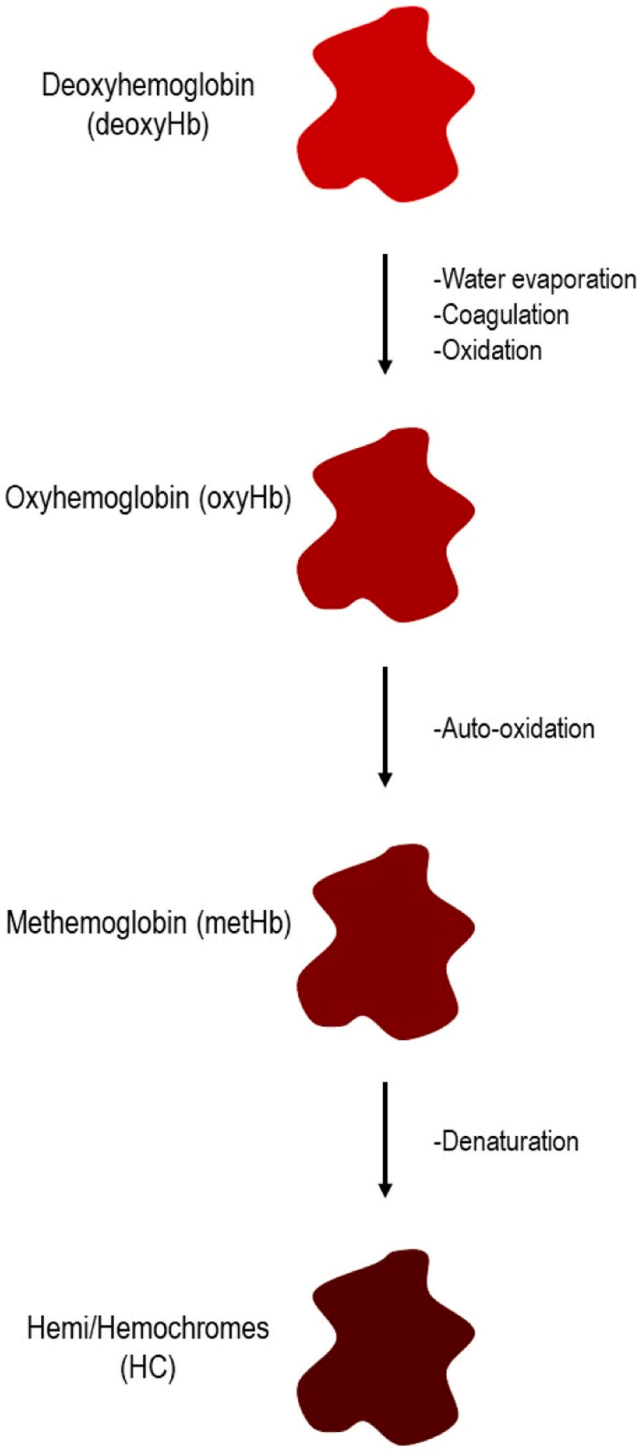

Fig. 1. Hemoglobin degradation process during ex vivo aging of blood.

2. Material and method

2.1. Sampling

First, to obtain the blood samples, the voluntary donor pricked their finger with a sterile McKesson 28 G safety lancet. While applying pressure around the finger to facilitate blood flow, the donor then deposited the blood on a piece of white cotton. All cotton pieces were cut from a white 100 % cotton T-shirt. All samples were freshly deposited immediately before being placed in the climatic chamber for the start of the aging process. For the sake of reproducibility, all samples were created using the same deposition method and they were all of similar quantity and size. The blood was also drawn from the same donor for all bloodstains.

2.2. Material and method

In order to optimize the analyses and assess the importance of the various factors, as well as the interactions between them, a factorial design of experiments (DoE) was created, consisting of 8 experiments

with two varying levels (maximum and minimum) of the three parameters to be analyzed, i.e., temperature, relative humidity and radiation (see Table 1).

Samples were left to age in a Memmert HPP110eco constant climate chamber, with the temperature inside the chamber adjustable from 5.0ºC to 70.0ºC ± 0.1ºC, and the relative humidity adjustable from 10.0 % to 90.0 % ± 0.5 %. The temperature range was chosen according to the conditions likely to be encountered at interior crime scenes, i.e., from 10ºC to 40ºC. Minimum and maximum relative humidity values were chosen according to the manufacturer's scale, indicating the humidity values achievable in the enclosure depending on temperature, i.e., from 25 % to 75 %. Two light sources were also added inside the enclosure to reproduce daylight conditions. The first was a 99 CRI Absolute Series D50 LED strip with a correlated color temperature (CCT) of 6500 K and an illumination of 3039 lux. The second was a realUV LED strip with a wavelength of 365 nm. Each experiment was left to age in the climatic chamber for 72 h with the corresponding parameters settings (See Table 1). On leaving the climatic chamber, the samples were immediately analyzed following the same sequence: 1) Photography under two halogen lamps at a 45° angle, 2) NIR (near infrared) spectroscopy analysis, 3) Raman spectroscopy analysis and 4) hyper-spectral imaging under the same halogen lamp setup as used for the photography. The camera used was a Nikon 5100, and the photos were then optimized using the Photoshop software. The device used for near-infrared measurements was a Viavi Solutions' MicroNIR OnSite-W, 950–1650 nm, equipped with a photodiode detector. Five replicates were measured for each sample. The NIR spectra were optimized using the Unscrambler software. The Raman instrument used was a Thermo Fisher DXR3 Raman microscope ranging from 400 to 2000 cm-1, equipped with a 532 nm laser. The laser power was set at 3 mW, with a 5-second exposure time and a 25 μm slit aperture. A 20X objective was used for the microscope and 5 replicas were measured for each sample. The Raman spectra were treated using the Unscrambler software. The hyper-spectral camera was a SpecimIQ, recording wavelengths from 400 to 1000 nm, with a spectral resolution of 7 nm. The spectral data obtained was then analyzed using the ENVI53 software, and an area of interest consisting of the 500 pixels located at the center of the blood trace was selected for each trace.

2.3. Data processing

Data processing was carried out entirely using Unscrambler software. For the MicroNIR data, a Savitsky-Golay first derivative of degree two polynomial with seven smoothing points was first applied to the entire replicas of the raw spectra. The first derivative was then followed by a standard normal variate (SNV) method over the entire dataset. For Raman data, SNV was first performed on all spectra obtained (5 replicas for each of the eight samples), followed by a detrending method (baseline correction). Finally, for the hyperspectral imaging data, a Savitsky-Golay first derivative of degree two polynomial with seven smoothing points was applied to the spectra of the 500 pixels making up the center of the trace for each of the eight blood samples, followed by SNV. Next, the pre-processed datasets were analyzed by principal component analysis (PCA) using the Unscrambler software, and the score-plots, loadings and explained variance graphs were obtained. The results of the PCA loadings were then used to select the most relevant variables (three per technique) to be included in the experimental design. Finally, Excel was used to create the experimental design matrices and to calculate the parameter influences.

Table 1
Factorial design of experiments of three parameters of two levels each.

Experiment	Temperature (°C)	Relative humidity (%)	Radiation
1	10	25	None
2	10	25	Max
3	10	75	None
4	10	75	Max
5	40	25	None
6	40	25	Max
7	40	75	None
8	40	75	Max

3. Results

3.1. Photography

Firstly, a photograph under a halogen lamp was acquired for each of the eight blood samples that had been left to age under different conditions (see Table 1). These photographs were used to observe the color differences between bloodstains that had been subjected to different environmental conditions. The eight processed photographs obtained were placed in order from lightest to darkest (Fig. 2).

The legend represents the experiment number (see Table 1) and the environmental conditions under which the blood trace in question was left to age. It can be seen that the four brightest-red, and therefore the lightest, traces are those for which the temperature was set at the lowest level, i.e., 10°C. On the other hand, the darkest, brownish traces are those that aged at 40°C. Among the four traces of the same temperature, a second separation is visible according to the radiation factor. Indeed, within the same temperature, the two darkest traces are those that have undergone radiation, both for those at 40°C and those at 10°C. Finally, between two traces left to age under the same radiation and temperature conditions, the trace with the lowest relative humidity is the darkest.

3.2. MicroNIR

Secondly, the samples were analyzed using Near-Infrared (NIR) spectroscopy. No significant variation between the five replicates acquired for the same sample were observed. The average NIR spectra were compiled on the following graph (Fig. 3) to compare between the eight different samples.

The graph compares the intensities of the absorbance bands present between each sample in the NIR range from 950 to 1650 nm. The bands highlighted represent those associated with compounds undergoing changes during blood degradation [8,17]. First, the blue bands correspond to the water present in the blood, at around 1450 nm. The red bands represent compounds present in erythrocytes. The methemoglobin and other proteins such as albumin and globulin, start to appear at around 1640 nm. It is possible to observe some variations in the intensity of the absorbance bands for the different samples in the spectra.

A principal component analysis (PCA) was conducted on the entirety of the NIR data, and the score plot obtained is shown in the following figure (Fig. 4).

The PCA score-plot shows that all samples are separated according to PC1 and PC2, except for samples 7 and 8, as some of the replicates overlap. Moreover, the eight samples appear to be separated into four subgroups of two, corresponding to the four score-plot quadrants according to PC1 and PC2. The subgroups correspond to the two samples with the same temperature and humidity conditions. Samples #3 and #4, i.e., those at 10°C and 75 % humidity, are in the upper right-hand quadrant (+/+). In the lower right-hand quadrant (+/-) are samples #1 and #2, i.e., those at 10°C and 25 % humidity. Samples #7 and #8, at 40°C and 75 % humidity, are in the upper left-hand quadrant (-/+). In the lower left-hand quadrant (-/-) are samples #5 and #6, i.e., those at 40°C and 25 % humidity. Therefore, PC1 separates the samples by temperature and PC2 separates the samples by relative humidity.

Finally, two design of experiments matrices were constructed using the MicroNIR spectroscopy data, in order to calculate the influence of the different parameters on two different response bands in the NIR range. The first table, Table 2 below, represents the design matrix for the peak at 1450 nm.

The response peak at 1450 nm was chosen since it is one of the peaks

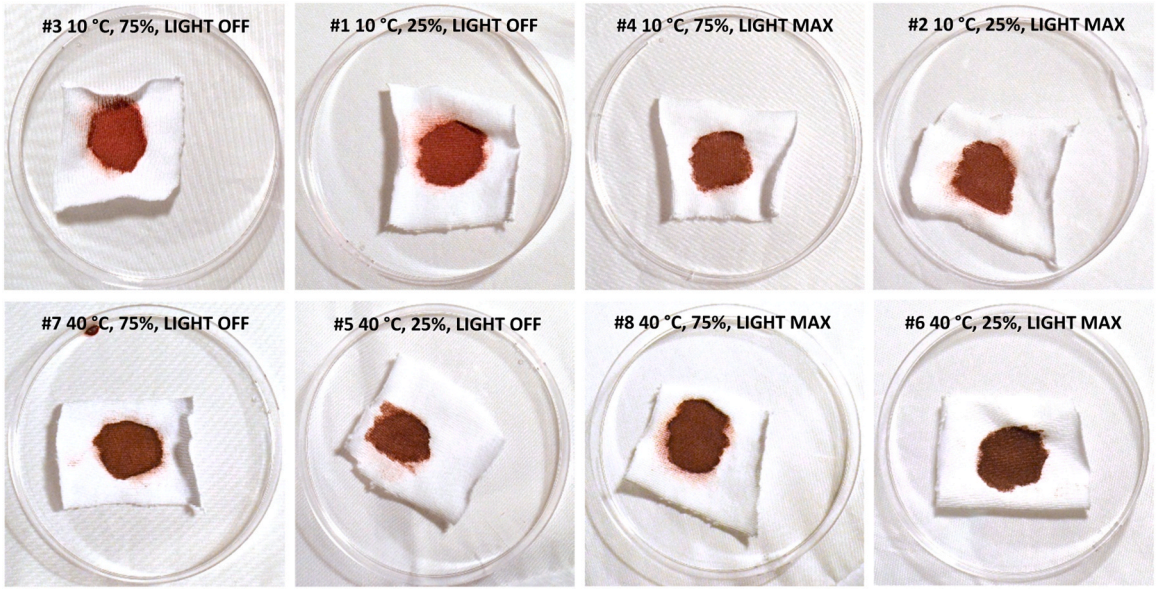

Fig. 2. Photographs of blood traces in ascending order from the brightest red to the darkest.

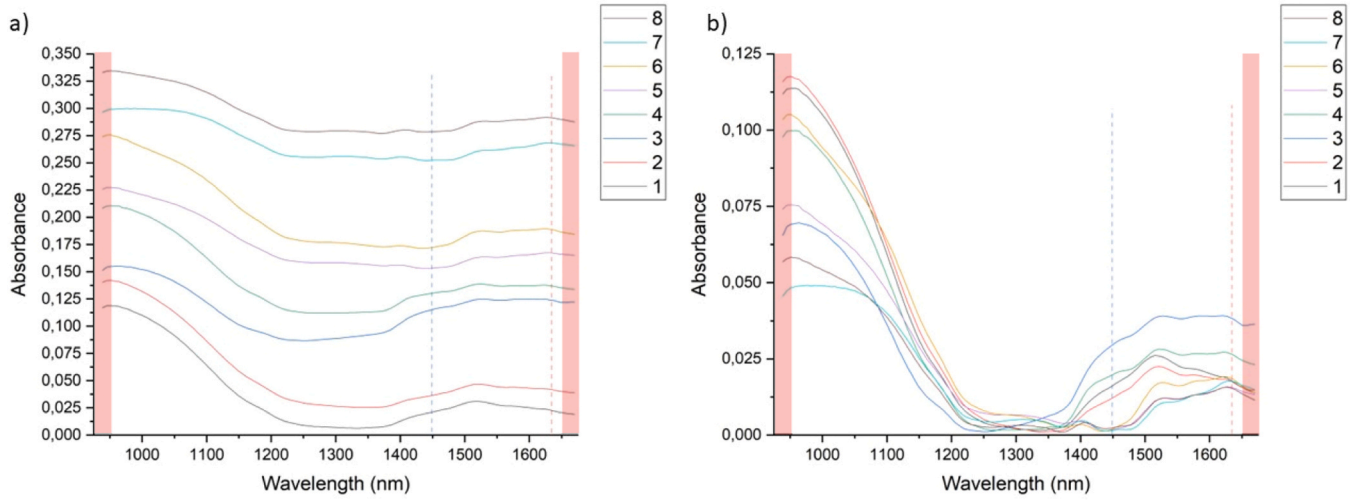

Fig. 3. Average MicroNIR spectra of each blood sample left to age under different conditions on a) an arbitrary scale and b) the same scale.

of water in blood, which varies during degradation [8]. The influence coefficients were calculated for each column (each parameter and interactions). Here is the equation used, using the first column (temperature) as an example:

$$b_A = \frac{A_1R_1 + A_2R_2 + A_3R_3 + A_4R_4 + A_5R_5 + A_6R_6 + A_7R_7 + A_8R_8}{8}$$

The b_A represents the influence coefficient for the parameter A, A_X represents the high or low setting of the parameter A for each experiment line, and R_X represents the response for each experiment.

The experimental design for the peak at 1450 nm of MicroNIR spectroscopy has determined that the two parameters that most affect this peak are temperature and relative humidity. The influence coefficient calculated for the first parameter (A, temperature) is −0.1195. This means that an increase in temperature between the low level at 10°C and the high level at 40°C reduces the intensity of the peak at 1450, i.e., a negative influence. The influence coefficient calculated for the second parameter (B, relative humidity), is + 0.1098. Unlike for the temperature, an increase in ambient relative humidity between a low level of 25 % and a high level of 75 % results in an increase in the peak at 1450 nm. For the radiation parameter (C), this influence coefficient is lower (-0.0460), meaning that the influence of solar radiation on the water peak in NIR spectroscopy is negligible compared with the other two parameters studied. As for the interactions between the parameters, these coefficients are also lower, demonstrating that there is no apparent interaction between the different parameters. The temperature (A) and relative humidity (B) parameters both have a significant influence, but the interaction between the two doesn't because the two parameters are not correlated, as one increases when the other diminishes.

The second table, Table 3 below, shows the design matrix for the peak at 1645 nm.

The peak at 1645 nm was chosen since it is associated with proteins present in human blood including methemoglobin, a more degraded conformation of hemoglobin, which begins after the first few hours of blood degradation [8,17]. The experimental design for the 1645 nm peak of the MicroNIR spectroscopy determined that there is one parameter in particular that affects methemoglobin formation more significantly than the others, namely the temperature. The influence coefficient calculated for this first parameter (A) is + 0.1208. This means that going from a low temperature level (10°C) to a high one

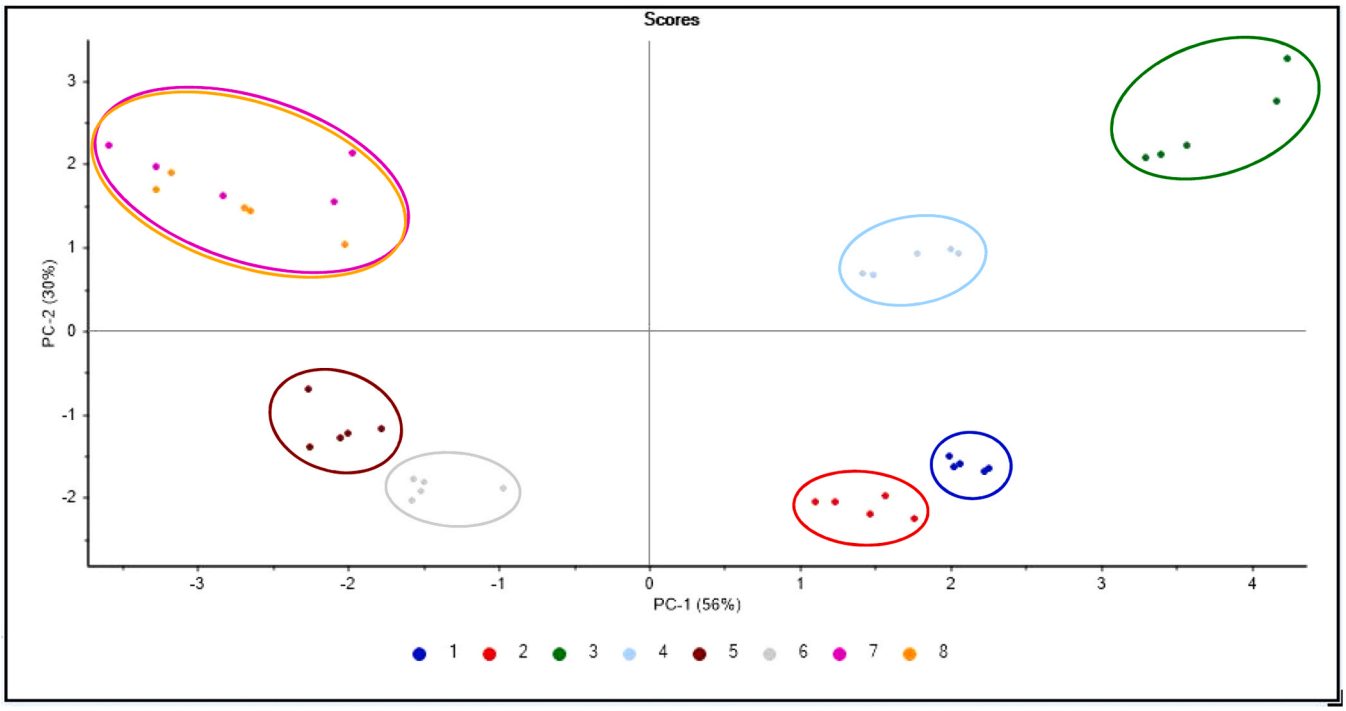

Fig. 4. Score plot of the principal component analysis of the MicroNIR spectra of the replicates of the eight different blood samples.

Table 2
Design of experiments matrix for the 1450 nm peak of the MicroNIR spectra of eight different blood samples.

	Linear			Interactions				Response
Experiment	A	B	C	AB	BC	AC	ABC	**y = 1450 nm**
1	-1	-1	-1	1	1	1	-1	0.3255339
2	-1	-1	1	1	-1	-1	1	0.2462499
3	-1	1	-1	-1	-1	1	1	0.6034435
4	-1	1	1	-1	1	-1	-1	0.212734
5	1	-1	-1	-1	1	-1	1	-0.0800153
6	1	-1	1	-1	-1	1	-1	-0.0244008
7	1	1	-1	1	-1	-1	-1	-0.0823677
8	1	1	1	1	1	1	1	-0.0392777
Influence	**-0.1195**	**0.1098**	-0.046	-0.0327	-0.0405	-0.0712	0.0369	

Table 3
Design of experiments matrix for the 1645 nm peak of the MicroNIR spectra of eight different blood samples.

	Linear			Interactions				Response
Experiment	A	B	C	AB	BC	AC	ABC	**y = 1645 nm**
1	-1	-1	-1	1	1	1	-1	-0.3310009
2	-1	-1	1	1	-1	-1	1	-0.2665178
3	-1	1	-1	-1	-1	1	1	-0.5308085
4	-1	1	1	-1	1	-1	-1	-0.2094643
5	1	-1	-1	-1	1	-1	1	-0.0507574
6	1	-1	1	-1	-1	1	-1	-0.1187604
7	1	1	-1	1	-1	-1	-1	-0.121142
8	1	1	1	1	1	1	1	-0.0801582
Influence	**0.1208**	-0.0219	0.0449	0.0137	0.0457	-0.0516	-0.0185	

(40°C) has the effect of increasing the intensity of the peak at 1645 nm. The influence coefficients calculated for the second parameter (B), relative humidity, and the third parameter (C), radiation, are lower than for the temperature parameter. The coefficients calculated for the interactions between parameters are also low, meaning that there is no significant interaction between the parameters.

3.3. Raman

The second spectroscopic analysis method used was Raman spectroscopy, and the same procedure as for MicroNIR was used to analyze the results. There was no variation between the five replicates acquired for each sample, and therefore the average spectrum of the replicates was obtained for each sample for the design of experiments calculations. All of the average Raman spectra were compiled on the same graph on Fig. 5 to observe the variations between the eight different samples.

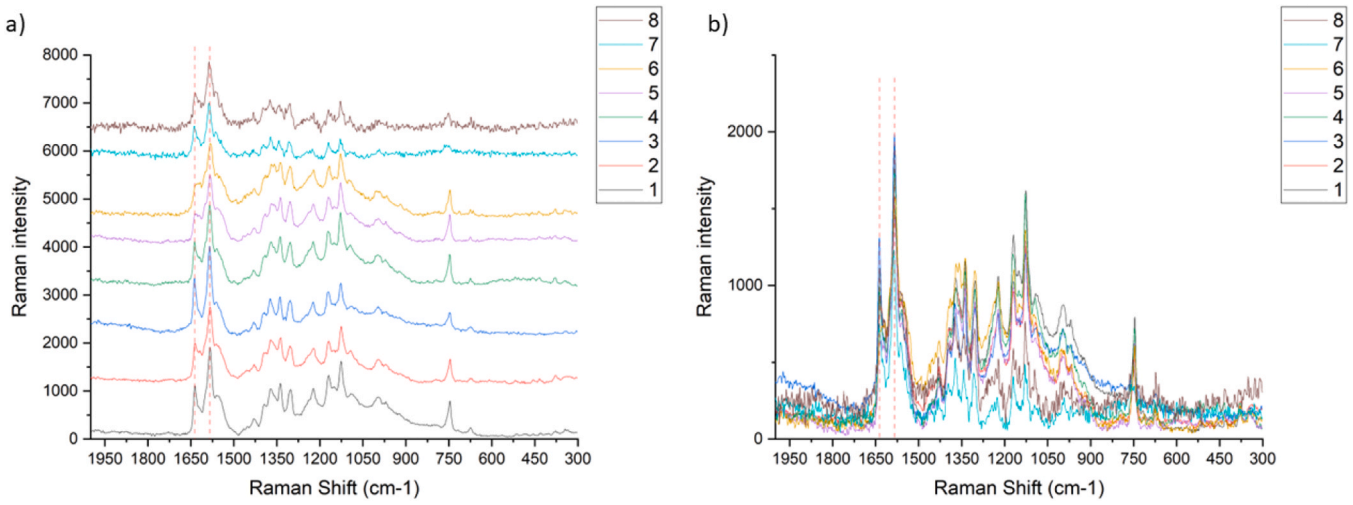

Fig. 5. Average Raman spectra of eight blood samples left to age under different environmental conditions on an a) arbitrary scale and b) the same scale.

The graph shows the average raw Raman spectra of all blood samples aged under different environmental conditions. Certain peaks have been highlighted in the figure using the red bands to illustrate peaks associated with changes during blood degradation [25,26]. Namely, the ones at 1648 cm-1 and 1585 cm-1. It is possible to see a decrease in the intensity of these peaks for certain samples, most notably samples #5, #6, #7 and #8, which are those that were left to age at high temperature (40°C), compared to the first four which were at low temperature (10°C). These peaks are attributed to the vibration of the heme skeleton in erythrocytes [25,26].

A principal component analysis (PCA) was also carried out for the Raman spectra, in order to visualize the separation of the different samples. Fig. 6 below shows the score-plot of the five replicates the eight samples as a function of PC1 and PC2.

According to PC1 and PC2, samples #1, #3, #6, #7 and #8, are all separated from the others, while there is an overlap of some replicates for samples #2, #4 and #5. Based on PC1, the horizontal axis, samples with low temperatures are on the positive side, while samples with high temperatures are on the negative side. There is no observable trend within the score-plot for relative humidity or radiation parameters.

Finally, two experimental design matrices were constructed on the Raman spectroscopy dataset, to be able to calculate the influence of different environmental parameters such as temperature, relative humidity and radiation on two Raman peaks that vary according to the level of degradation. The first table, Table 5 below, represents the design matrix for the peak at 1648 cm-1.

The response at 1648 cm-1 was chosen since this is a peak that varies during blood degradation and illustrates the distortions of the porphyrin ring and the spin state of the iron atom in hemoglobin [26]. The experimental design for the peak at 1648 cm-1 of the Raman spectroscopy determined that the environmental conditions parameter with the greatest influence on this peak is temperature (A). The influence coefficient calculated for this parameter is −0.1239. This means that the increase in temperature between the low level at 10°C and the high level

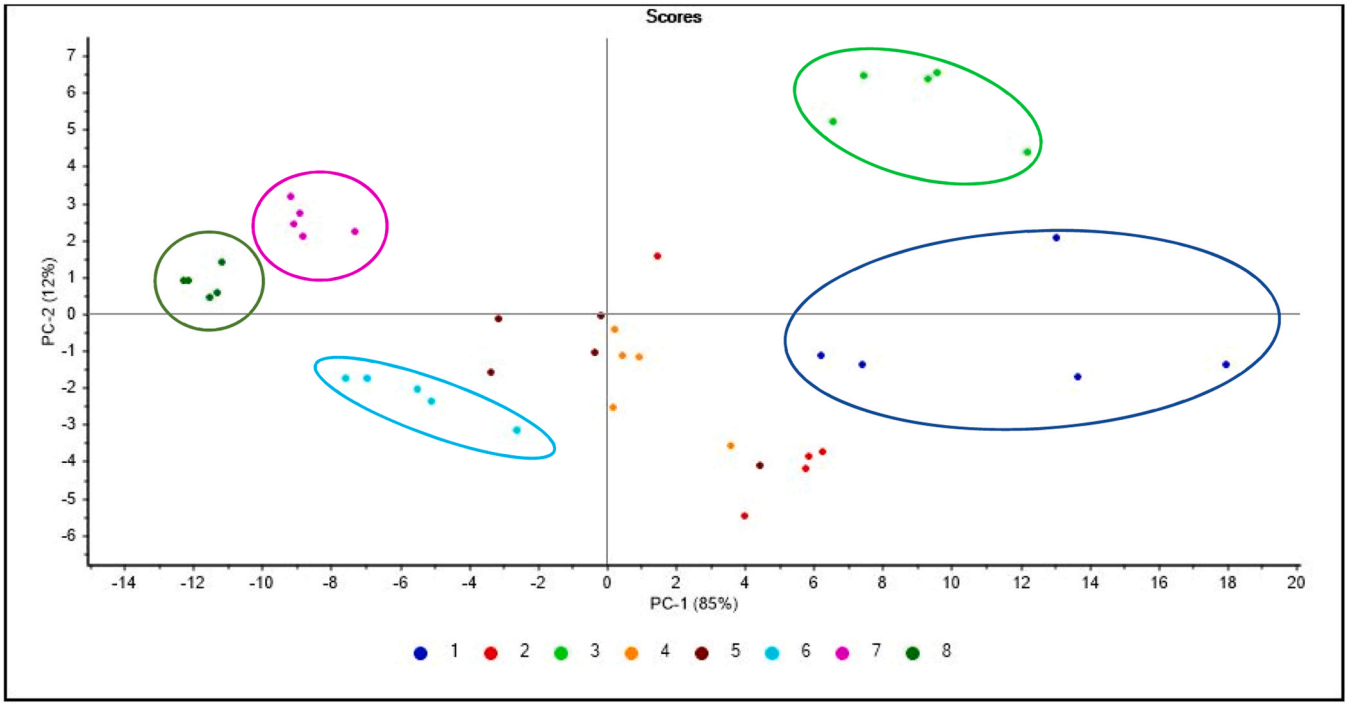

Fig. 6. Score plot of the principal component analysis of the Raman spectra of the replicates of the eight different blood samples.

Table 4
Design of experiments matrix for the 1648 cm-1 peak of the Raman spectra of eight different blood samples.

	Linear			Interactions				Response
Experiment	A	B	C	AB	BC	AC	ABC	y = 1648
1	-1	-1	-1	1	1	1	-1	0.422007
2	-1	-1	1	1	-1	-1	1	0.36931
3	-1	1	-1	-1	-1	1	1	0.376399
4	-1	1	1	-1	1	-1	-1	0.263841
5	1	-1	-1	-1	1	-1	1	0.118653
6	1	-1	1	-1	-1	1	-1	0.094371
7	1	1	-1	1	-1	-1	-1	0.143954
8	1	1	1	1	1	1	1	0.083449
Influence	**-0.1239**	-0.0171	-0.0313	0.0207	-0.0120	0.0101	0.0030	

Table 5
Design of experiments matrix for the 1585 cm-1 peak of the Raman spectra of eight different blood samples.

	Linear			Interactions				Response
Experience	A	B	C	AB	BC	AC	ABC	y = 1585
1	-1	-1	-1	1	1	1	-1	1.270684
2	-1	-1	1	1	-1	-1	1	1.051273
3	-1	1	-1	-1	-1	1	1	0.894748
4	-1	1	1	-1	1	-1	-1	0.760168
5	1	-1	-1	-1	1	-1	1	0.596069
6	1	-1	1	-1	-1	1	-1	0.460812
7	1	1	-1	1	-1	-1	-1	0.310498
8	1	1	1	1	1	1	1	0.205687
Influence	**-0.3983**	0.0155	-0.0917	**0.1822**	-0.0368	-0.0032	-0.0580	

at 40°C has a negative influence on the peak at 1648 cm-1, reducing its intensity. For the parameters of relative humidity (B) and radiation (C), this influence coefficient is lower, i.e., −0.0171 for humidity and −0.0313 for radiation, so the influence of relative humidity and radiation on this blood peak in Raman spectroscopy is negligible compared with temperature. As for the interactions between the parameters, these coefficients are also low, meaning that there is no particular interaction between the parameters.

The second table, Table 5 below, represents the design of experiments matrix for the peak at 1585 cm-1.

The response peak at 1585 cm-1 was chosen as the second response as it is also a Raman peak associated with distortions of the porphyrin ring and the spin state of the iron atom in hemoglobin [26]. The experimental design for the peak at 1585 cm-1 of the Raman spectroscopy determined that the parameter with the greatest influence on this peak is also the temperature (A). The calculated influence coefficient for this parameter is −0.3983. This means that as temperature increases between the low level at 10°C and the high level at 40°C, the intensity of the peak at 158 cm-1 decreases. Temperature therefore has a negative influence on this peak. For the relative humidity (B) and radiation (C) parameters, this influence coefficient is lower, at −0.0155 for humidity and −0.0917 for radiation. The influence of relative humidity and radiation on this blood peak in Raman spectroscopy is small and therefore negligible compared to the influence of temperature. As for interactions between parameters, there is a possible interaction between temperature and relative humidity (RH), since the calculated influence coefficient was larger, at 0.1822. This means that high temperature (40°C) coupled with high humidity (75 %) has a positive influence on the Raman peak at 1585 cm-1. For the other interactions (BC, AC and ABC), the coefficients are low, meaning that there is no particular interaction between the parameters.

3.4. Hyperspectral imaging

The last spectroscopic analysis method used was hyperspectral imaging. A total of 500 spectra covering the center of the bloodstain's hypercubes of the hyperspectral image was selected for each sample, as shown in Fig. 7 below.

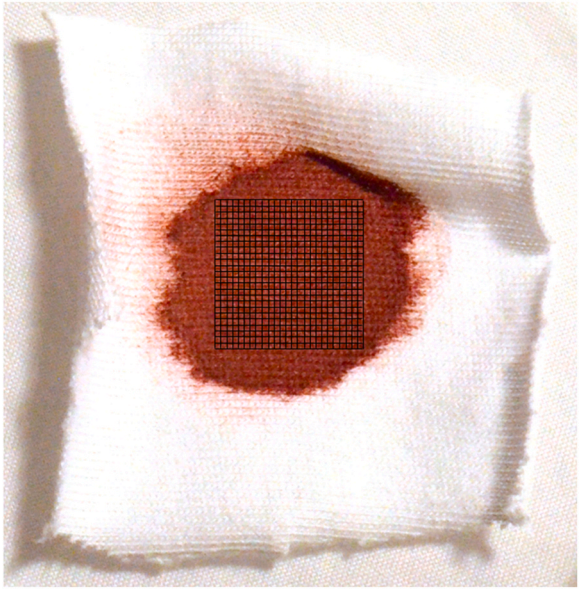

Fig. 7. Schematic representation of the surface covered by the 500 hypercubes of the hyperspectral imaging on the bloodstain.

The average spectrum obtained from the 500 spectra acquired was calculated from the central region of the hyperspectral image of each blood sample. All of the average hyperspectral spectra were compiled on the same graph on Fig. 8 to observe the variations between the eight different samples.

Fig. 8 shows the average raw hyperspectral imaging spectra of all blood samples aged under different environmental conditions. The wavelengths highlighted on the figure with red lines illustrate the bands that varied between samples. These are situated at 550 nm, 580 nm, and between 650 and 700 nm. It is possible to see a variation in the reflectance intensity of these peaks between the different samples. The two sunken areas around 550 and 580 nm are attributed to hemoglobin in

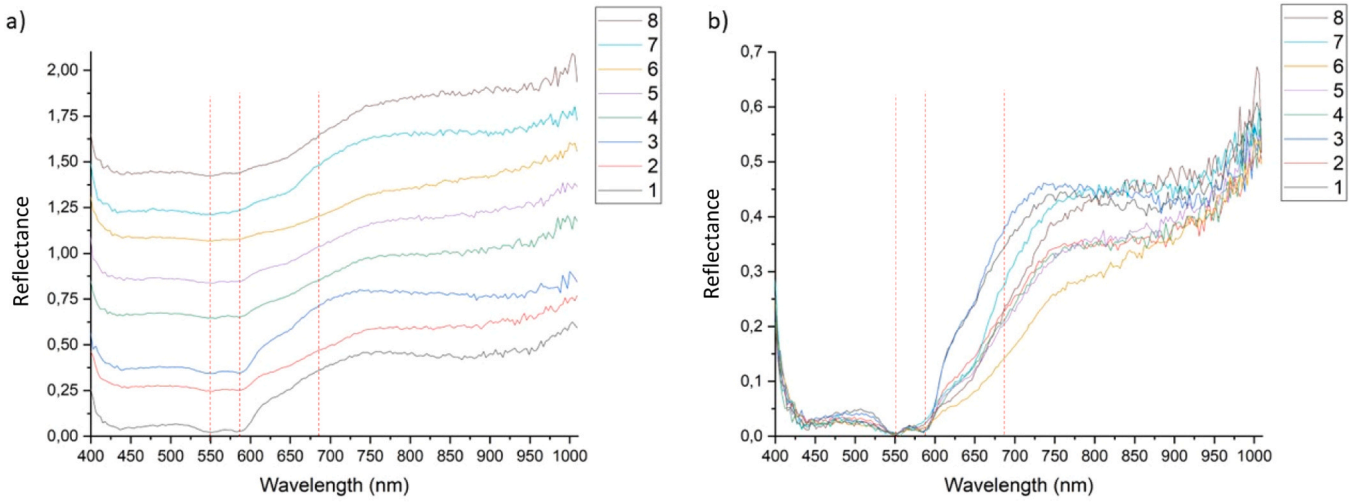

Fig. 8. Average hyperspectral imaging spectra of eight blood samples left to age under different environmental conditions on a) an arbitrary scale and b) the same scale.

the blood, more specifically the α and β bands of oxyhemoglobin [9,27,28]. The area between 650 and 700 nm, i.e. the red region of the spectrum, is associated with the change in color of the blood, ranging from a bright red to dark brown [27,29].

A principal component analysis (PCA) was also carried out on the hyperspectral imaging data. This enabled the separation of the different samples to be visualized. Fig. 9 below shows the score plot of the 500-pixel spectra making up the blood trace of each of the eight samples according to PC1 and PC2.

According to the first two principal components, all of the samples are separated from each other, except for a very slight overlap between samples #2 and #4. On the horizontal axis, according to PC1, the samples left to age at a low temperature tend to be on the right-hand side of the score-plot (positive), while samples at a high temperature tend to be on the left-hand side (negative). Only sample #4, which was at a temperature of 10°C, is found in the center, in-between the positive and negative sides. There is no visually observable trend with the score-plot for the relative humidity or radiation parameters. The PCA score-plot also reveals the low intra-variability within a single trace. Indeed, the 500 different spectra represented for each sample are all highly concentrated, and very few replicas are further away from the others.

Finally, two experimental design matrices were also created for the hyperspectral imaging dataset, in order to calculate the influence of the different environmental parameters such as temperature, relative humidity and radiation on two variable bands depending on the level of degradation. The first table, Table 6 below, represents the design matrix for the area between 650 and 700 nm.

The response peak at 675 nm was chosen as it is a peak that varies during blood degradation. As the blood further degrades, the color changes from a bright red to a dark brown, resulting in a decrease in the slope between 650 and 700 nm [27,29]. The experimental design for the 675 nm response of hyperspectral imaging has determined that the two parameters of environmental conditions with the greatest influence on this band are the temperature (A) and the electromagnetic radiation (C). For the first parameter, temperature, the calculated influence coefficient is −0.8582. Temperature therefore has a negative influence on reflectance intensity at 675 nm. This means that as the temperature increases from a low of 10°C to a high of 40°C, the intensity at 675 nm decreases. For the radiation factor (C), this influence coefficient is −0.7012. Radiation therefore varies the band at 675 nm in the same way as

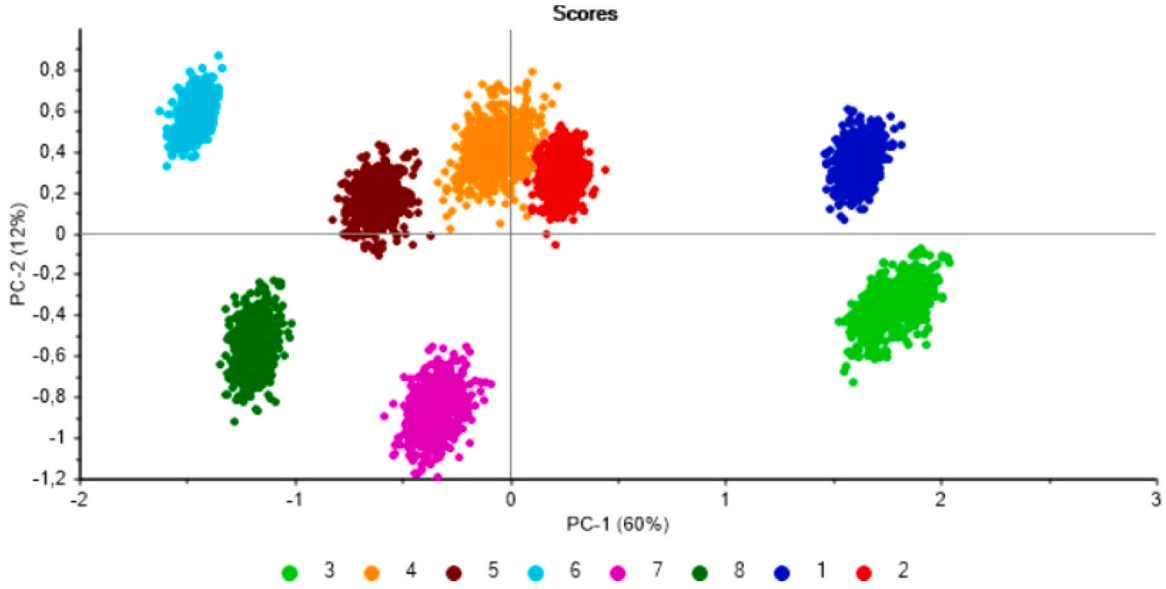

Fig. 9. Score plot of the principal component analysis of the hyperspectral imaging spectra of the replicates of the eight different blood samples.

Table 6
Design of experiments matrix for the 675 nm response of the hyperspectral imaging spectra of eight different blood samples.

	Linear			Interactions				Response
Experience	A	B	C	AB	BC	AC	ABC	y = 675 nm
1	-1	-1	-1	1	1	1	-1	0.36300868
2	-1	-1	1	1	-1	-1	1	0.16738126
3	-1	1	-1	-1	-1	1	1	0.42901547
4	-1	1	1	-1	1	-1	-1	0.1531816
5	1	-1	-1	-1	1	-1	1	0.08765044
6	1	-1	1	-1	-1	1	-1	-0.01500594
7	1	1	-1	1	-1	-1	-1	0.15439324
8	1	1	1	1	1	1	1	0.02731286
Influence	**-0.8582**	0.1609	**-0.7012**	0.0573	-0.1046	0.2417	0.0558	

temperature, i.e., negatively. The addition of 99CRI and UV electromagnetic radiation therefore also results in a lower reflectance at 675 nm. The influence of relative humidity is lower than for the other two parameters, at 0.1609, but it is positive. As for the interactions between the parameters, the coefficients are also lower, meaning that there is no particular interaction between the parameters.

The second table, Table 7 below, represents the design matrix for the 580 nm peak of hyperspectral imaging.

The 580 nm response was chosen as it is also a band that varies during blood degradation. The sunken area is associated with the presence of oxyhemoglobin, and it should even out as the oxyhemoglobin further degrades [9,27,28]. The experimental design for the 580 nm response of hyperspectral imaging determined that the two parameters of environmental conditions with the greatest influence on this band are also temperature (A) and electromagnetic radiation (C). However, unlike the peak at 675 nm, these two parameters positively influence the response to this band. For temperature, the calculated influence coefficient is 1.0931. So, as the temperature rises from a low of 10°C to a high of 40°C, there is an increase in reflectance at 580 nm. The same observation applies to the radiation factor (C) since its influence coefficient is + 0.8323. Radiation therefore also leads to an increase in reflectance at 580 nm. The influence of humidity is negligible compared to temperature and radiation, at −0.1457, but it is negative. The experimental design at 580 nm also revealed that the interactions between the parameters were negligible since the coefficients are also lower.

4. Discussion

First, it was possible to observe a trend present between the color of the bloodstains and the environmental parameters of temperature, relative humidity, and electromagnetic radiation within the climatic chamber during the aging period of the eight samples. It was observed that the four samples aged under low temperature conditions, i.e., 10°C, were the brightest red, while the four samples with a dark brown color were those aged under high temperature conditions, i.e., 40°C. Within these two groups of four samples, the two darkest were those subjected to electromagnetic radiation during aging. Finally, a lower relative humidity of 25 % resulted in a darker bloodstain than a high relative humidity of 75 %, between two stains that had the same temperature and radiation conditions. A dark brown color indicates a more advanced level of blood degradation. Thus, increasing the temperature between 10°C and 40°C accelerates ex vivo degradation. This is also the case for the addition of radiation, since samples left to age under UV and 99CRI LED strips are darker than those left in complete darkness. The opposite was observed for relative humidity. Increasing humidity to 75 % resulted in redder stains than the low level of 25 %, which in turn resulted in browner stains. These observations are in line with what can be expected from a theoretic point of view. In fact, increasing ambient humidity leads to the hydration of the bloodstain and may prevent the final degradation step, i.e., conversion of methemoglobin to hemichromes [21,22]. High temperature and radiation act as catalysts for the degradation process, particularly for the auto-oxidation of oxyhemoglobin to methemoglobin, which has also been observed.

Secondly, the blood samples were analyzed using NIR spectroscopy, in a range of wavelengths going from 950 nm to 1650 nm. It was first observed that there was a low intra-variability within the same bloodstain, as there was no variation between the replicates acquired at different places on the same sample. There were several variations between the pretreated spectra of the samples that were left to age under different environmental conditions. The design of experiments for the NIR data showed that the two parameters that were the most influent on the peak variations were the temperature and the relative humidity. An increase in temperature increased the intensity of the peak at 1645 nm and an increase in relative humidity increased the intensity of the peak at 1450 nm, which is associated to the presence of water [8]. Since one of the first stages of bloodstain degradation is the evaporation of water, higher water peaks can mean a less degraded blood sample [30,31].

The samples were also analyzed using Raman spectroscopy. Once again, a very low intra-variability was observed within the same sample, but an inter-variability was observed between the pretreated Raman spectra of the eight samples left to age under different environmental conditions. A design of experiments was created once again to determine which parameters had the biggest influence on the peak variations. For the two peaks analyzed, which were the one at 1648 cm^{-1} and the one at 1585 cm^{-1}, it was only the temperature that seemed to influence the variations observed, and it was determined that an increase in temperature had the effect of decreasing the intensity of the peaks. These peaks are associated to the vibration of the heme skeleton in hemoglobin, and

Table 7
Design of experiments matrix for the 580 nm response of the hyperspectral imaging spectra of eight different blood samples.

	Linear			Interactions				Response
Experience	A	B	C	AB	BC	AC	ABC	y = 580 nm
1	-1	-1	-1	1	1	1	-1	-0.87920207
2	-1	-1	1	1	-1	-1	1	-0.65964667
3	-1	1	-1	-1	-1	1	1	-0.9259263
4	-1	1	1	-1	1	-1	-1	-0.57942021
5	1	-1	-1	-1	1	-1	1	-0.52885524
6	1	-1	1	-1	-1	1	-1	-0.35707681
7	1	1	-1	1	-1	-1	-1	-0.57978931
8	1	1	1	1	1	1	1	-0.48537393
Influence	**1.0931**	-0.1457	**0.8323**	-0.2127	0.0496	-0.2999	-0.2043	

they decrease in intensity during the degradation process [26].

Lastly, the eight samples were also analyzed using hyperspectral imaging. Since an area of 500 pixels in the center of the bloodstain was selected for each sample, 500 different hyperspectral spectra were analyzed for each of the eight bloodstains. It was then observed that the intra-variability within these spectra was very low. However, there were variations between the average spectra of the different aged samples. A design of experiments was also created to observe how the different environmental parameters influence the variations in the spectra. The bands analyzed were the ones at 675 nm and 580 nm. For both of these wavelengths, the two parameters that were the most influent were the temperature and the radiation. For the area at 675 nm, mainly associated with the change in color [27,29], the increase in temperature and radiation decreased the reflectance intensity. For the band at 580 nm, which is associated to the hemoglobin signal in blood [9,27,28], the reflectance is higher when there is an increase in the temperature and radiation.

It was possible to see that the spectroscopic methods used, as well as being portable, were complementary to each other. Indeed, they all allowed to obtain information on the effect of temperature, but only with NIR spectroscopy was the effect of relative humidity observed, and only with hyperspectral imaging was the effect of radiation observed. Therefore, combining these methods can provide a full understanding of the three environmental parameters studied.

Although this project has provided information on the influence of environmental conditions on the degradation of blood traces, a few limitations remain. One of the limitations of the method is in fact the limits of the range of environmental conditions evaluated. The maximum and minimum levels were chosen to obtain an experimental design adapted to environmental conditions at the extremes allowed by the capabilities of the climatic chamber used, instead of a model that is too precise for average environmental conditions and no longer suitable when moving away from this average. However, it is possible to be confronted to environmental conditions beyond these at an exterior crime scene. The conditions evaluated are therefore suitable for indoor scenes, but not for certain outdoor scene conditions. For example, we would need to evaluate the degradation of blood traces stored in sub-zero temperatures to represent winter conditions. Also, the samples analyzed in this experiment were controlled samples, all deposited on the same substrate and in the same way. Traces collected at crime scenes, however, are rather left unintentionally under chaotic conditions, and are therefore often imperfect, of poor quality, or even contaminated. In this experiment, blood from a single donor was used. Additional experiments with multiple donors are currently ongoing. In particular cases, it is possible that certain diseases affecting blood coagulation, for example, could influence the dynamics of blood degradation [4,32], which could not be verified here. Another parameter influencing the ex vivo degradation of blood is the type of substrate on which it is deposited. In this experiment, only white cotton was used as a substrate. However, some substrates that present a strong background signal can potentially mask the blood signal when analyzed by the various spectroscopic methods [8,17,18,27]. A comparison between porous and non-porous substrates would be particularly interesting as it might influence degradation dynamics by affecting water evaporation time.

5. Conclusion

In conclusion, the influence of environmental parameters - temperature, relative humidity and radiation - on the degradation of blood traces deposited on white cotton was analyzed. This was made possible by a factorial experimental design with three environmental factors that varied between two levels, a minimum and a maximum. These two extremes represent the range of conditions likely to be found at indoor crime scenes, as opposed to an overly precise model that would not be adapted to changing environmental conditions. It was also possible to determine which spectroscopic analysis techniques were appropriate for analyzing the degradation of blood on cotton, and what information each technique provides about the trace. The project also determined the appropriate data processing for blood trace analysis, for each spectroscopic analysis method. This project also demonstrates that the spectroscopic methods used are complementary, since the three together provide information on degradation as a function of all the parameters studied. This project has also enabled us to determine how the sample's environment affects its degradation dynamics: increasing temperature accelerates the rate of degradation, increasing relative humidity slows the rate of degradation, and the presence of electromagnetic radiation accelerates the rate of degradation. In addition to providing information on how each environmental parameter affects the level of degradation of blood deposited on cotton, it was also possible to determine which regions should be targeted on the different spectra for the assessment of blood trace degradation. Indeed, for each of the techniques, it was possible to identify important peaks whose intensity and appearance vary according to the level of degradation reached. Finally, this project has enabled us to optimize and validate blood degradation analysis methods that are also portable devices. Indeed, the use of portable techniques allows for measurements to be taken directly at the crime scene at the moment of the detection of the trace, a major advantage for blood degradation analysis and dating. Taking measurements directly at the scene avoids the time spent transporting and storing the traces prior to laboratory analysis, as well as the variable environmental conditions they will undergo during this process, all of which could affect the level of degradation of the trace. These measurements can also be taken directly on the surface on which the trace is found, thus avoiding trace collection techniques such as the use of a wet cotton swab, which can affect the degradation process.

There are still many possible approaches and important parameters to be studied for blood degradation. First of all, assessing the effect of environmental conditions on the degradation process is only one of the three major influencing factors, the other two being the influence of the substrate and the variations in blood composition [1]. It will therefore be imperative to also analyze these two other parameters, in order to take into account these particularities of the trace, which is not a controlled sample.

CRediT authorship contribution statement

Laurianne Huard: Writing – original draft, Visualization, Software, Methodology, Investigation, Funding acquisition, Formal analysis. **Cyril Muehlethaler:** Writing – review & editing, Supervision, Resources, Project administration, Conceptualization. **Frank Crispino:** Supervision, Project administration.

Declaration of Competing Interest

There are no conflict of interest to declare from the authors.

Acknowledgments

We are grateful to the NSERC Canada Graduate Doctoral and Master's Scholarship, and to the FRQNT Master's Training Scholarship for financial support of this project, as well as to Andy Bécue from the University of Lausanne the warm welcome and his help during a mobility stay and stimulating discussions on the subject.

References

[1] G. Zadora, A. Menżyk, In the pursuit of the holy grail of forensic science – Spectroscopic studies on the estimation of time since deposition of bloodstains, TrAC Trends Anal. Chem. 105 (2018).
[2] S.H. James, P.E. Kish, T.P. Sutton, Principles of Bloodstain Pattern Analysis. Theory and Practice, 1st edition, CRC Press, 2005.

[3] R.H. Bremmer, et al., Forensic quest for age determination of bloodstains, Forensic Sci. Int. 216 (1-3) (2012) 1–11.
[4] K.C. Doty, C.K. Muro, I.K. Lednev, Predicting the time of the crime: bloodstain aging estimation for up to two years, Forensic Chem. 5 (2017) 1–7.
[5] H. Lin, et al., Estimation of the age of human bloodstains under the simulated indoor and outdoor crime scene conditions by ATR-FTIR spectroscopy, Sci. Rep. 7 (1) (2017) 13254.
[6] A. Menżyk, et al., Toward a novel framework for bloodstains dating by Raman spectroscopy: how to avoid sample photodamage and subsampling errors, Talanta 209 (2020) 120565.
[7] B. Li, et al., The estimation of the age of a blood stain using reflectance spectroscopy with a microspectrophotometer, spectral pre-processing and linear discriminant analysis, Forensic Sci. Int. 212 (1) (2011) 198–204.
[8] G.J. Edelman, et al., Identification and age estimation of blood stains on colored backgrounds by near infrared spectroscopy, Forensic Sci. Int. 220 (1-3) (2012) 239–244.
[9] G. Edelman, T.G. van Leeuwen, M.C. Aalders, Hyperspectral imaging for the age estimation of blood stains at the crime scene, Forensic Sci. Int. 223 (1-3) (2012) 72–77.
[10] P. Thanakiatkrai, A. Yaodam, T. Kitpipit, Age estimation of bloodstains using smartphones and digital image analysis, Forensic Sci. Int. 233 (1-3) (2013) 288–297.
[11] S.S. Kind, D. Patterson, G.W. Owen, Estimation of the age of dried blood stains by a spectrophotometric method, Forensic Sci. 1 (1) (1972) 27–54.
[12] Shine, S.M., et al. The applicability of fluorescence lifetime to determine the time since deposition of biological stains. 2017.
[13] E. Botoniic-Sehic, et al., Forensic Application of Near-Infrared Spectroscopy. Aging of Bloodstains. Spectroscopy, (Santa Monica), 2009, p. **24**.
[14] D. Patterson, Use of reflectance measurements in assessing the colour changes of ageing bloodstains, Nature 187 (4738) (1960) 688–689.
[15] H. Inoue, et al., A new marker for estimation of bloodstain age by high performance liquid chromatography, Forensic Sci. Int 57 (1) (1992) 17–27.
[16] Y. Fujita, et al., Estimation of the age of human bloodstains by electron paramagnetic resonance spectroscopy: long-term controlled experiment on the effects of environmental factors, Forensic Sci. Int. 152 (1) (2005) 39–43.
[17] N. Stritt, *L'estimation de l'âge d'une trace de sang: Quels sont les défis?*. École des sciences criminelles Université de Lausanne, Lausanne, 2014.
[18] T. Bergmann, F. Heinke, D. Labudde, Towards substrate-independent age estimation of blood stains based on dimensionality reduction and k-nearest neighbor classification of absorbance spectroscopic data, Forensic Sci. Int. 278 (2017) 1–8.
[19] C. Weyermann, O. Ribaux, Situating forensic traces in time, Sci. Justice 52 (2) (2012) 68–75.
[20] F. Ramsthaler, et al., Effect of anticoagulation therapy on drying times in bloodstain pattern analysis, Int J. Leg. Med 131 (4) (2017) 955–961.
[21] O.K. Baskurt, H.J. Meiselman, Blood rheology and hemodynamics, Semin Thromb. Hemost. 29 (5) (2003) 435–450.
[22] J.M. Rifkind, et al., Detection, formation, and relevance of hemichromes and hemochromes, Methods Enzymol 231 (1994) 449–480.
[23] M.F. Colombo, R. Sanches, Hydration-dependent conformational states of hemoglobin: equilibrium and kinetic behavior, Biophys. Chem. 36 (1) (1990) 33–39.
[24] K.C. Doty, G. McLaughlin, I.K. Lednev, A Raman "spectroscopic clock" for bloodstain age determination: the first week after deposition, Anal. Bioanal. Chem. 408 (15) (2016) 3993–4001.
[25] K. Virkler, I.K. Lednev, Raman spectroscopic signature of blood and its potential application to forensic body fluid identification, Anal. Bioanal. Chem. 396 (1) (2010) 525–534.
[26] B.R. Wood, D. McNaughton, Raman excitation wavelength investigation of single red blood cells in vivo, J. Raman Spectrosc. 33 (7) (2002) 517–523.
[27] V. Choumilov, *The influence of the substrate on the characterisation and visualisation of blood using hyperspectral imaging*. École des sciences criminelles, Université de Lausanne, Lausanne, 2016.
[28] M. Zulfiqar, et al., Hyperspectral imaging for bloodstain identification, Sensors 21 (9) (2021) 3045.
[29] S. Cadd, et al., A comparison of visible wavelength reflectance hyperspectral imaging and Acid Black 1 for the detection and identification of blood stained fingerprints, Sci. Justice 56 (4) (2016) 247–255.
[30] B. Faivre, et al., Hemoglobin autooxidation/oxidation mechanisms and methemoglobin prevention or reduction processes in the bloodstream. Literature review and outline of autooxidation reaction, Artif. Cells Blood Substit. Immobil. Biotechnol. 26 (1) (1998) 17–26.
[31] A.M. Stadler, et al., Hemoglobin dynamics in red blood cells: correlation to body temperature, Biophys. J. 95 (11) (2008) 5449–5461.
[32] Larkin, B.A.J. Bloodstain pattern analysis: scratching the surface. 2015..